

Effects of disorder on a smectic-*A*–nematic phase transition

S. Larochelle,¹ M. Ramazanoglu,¹ and R. J. Birgeneau^{1,2}

¹*Department of Physics, University of Toronto, Toronto, Ontario, Canada M5S 1A7*

²*Department of Physics, University of California, Berkeley, California 94720, USA*

(Received 13 January 2006; published 20 June 2006)

Using x-ray scattering, we have studied the nematic to smectic-*A* phase transition of the liquid crystal butyloxybenzilidene-octylaniline confined in an aerosil network. We find that the disorder introduced by the aerosil network destroys the long-range nature of the phase transition, and that the transition becomes similar to that observed in a finite-size system, with finite low-temperature correlation lengths of the ordered moments and a power-law behavior of the order parameter with respect to the reduced temperature observable in a limited temperature range. We also show evidence for a systematic evolution of the effective order parameter critical exponent β with increasing disorder.

DOI: [10.1103/PhysRevE.73.060702](https://doi.org/10.1103/PhysRevE.73.060702)

PACS number(s): 61.30.Pq, 61.30.Eb, 64.70.Md, 61.10.Eq

I. INTRODUCTION

The study of phase transitions in the presence of disorder is of fundamental interest in condensed matter physics as some level of disorder is present in any naturally occurring thermodynamical system. In fluids, disorder can be introduced in a controlled way by confining the fluid in a random porous medium. The density of the porous medium can be used as a parameter to characterize the strength of the disorder. Numerous studies of aerogel-confined superfluid helium [1,2] and binary liquids [3] have been reported. For liquid crystals, confinements in aerogels [4,5] and aerosil gels [6–12] have been tried. Aerogels are rigid chemically bonded silica gels while aerosil gels are thixotropic, hydrogen-bonded silica gels. Because of the weaker bonding, aerosil gels cause less severe disorder at a given density than aerogels. The aerosil gel appears to be partially restructured when the liquid crystal molecules order at low temperature [8,13]. This implies a partial annealing of the disorder.

In the absence of aerosil particles, the smectic-*A* phase of liquid crystals is characterized by a two-component order parameter in a three-dimensional space (3D *XY* symmetry). The silica nanoparticles of the gel form a random network that provides pinning centers for the liquid crystal molecules. This perturbs both the orientation of the nematic director and the phase of the charge density wave [14], and causes the disappearance of the long-range nature of the smectic-*A* phase of pure liquid crystals [5,9,10,12]. At low aerosil density, the smectic order correlation lengths are quite long and it is possible to observe a relatively well-defined transition. Since the correlation lengths of the smectic order never become infinite, this is not strictly speaking a thermodynamical phase transition, but the term is used in this Rapid Communication to describe the change to an ordered state of finite extent.

The effects of aerosil gel confinement on the nematic to smectic-*A* transition have been studied in detail with x-ray scattering in two liquid crystals: octylcyanobiphenyl (8CB) [9,10,13] and octyloxycyanobiphenyl (8OCB) [12]. These two liquid crystals are polar materials and they have partial bilayer smectic phases. As a continuation of this study, we looked at the effect of aerosil networks on

a nonpolar material with a monomeric smectic-*A* phase, *N*-4-*n*-butyloxybenzilidene-4'-*n*-octylaniline (4O.8) [6,15]. Pure 4O.8 shows the following phases:

$$\text{CrK} \text{ — } \text{CrB} \text{ — } \text{SmA} \text{ — } \text{N} \text{ — } \text{I}$$

$$311.2 \text{ K} \quad 322.6 \text{ K} \quad 336.9 \text{ K} \quad 352 \text{ K}$$

where CrK, CrB, SmA, N, and I designate the crystalline-*K*, crystalline-*B*, smectic-*A*, nematic, and isotropic phases, respectively. The nematic to smectic-*A* transition is second order and is characterized by the critical exponents $\alpha=0.134(15)$, $\gamma=1.31(2)$, $\nu_{\parallel}=0.70(1)$, and $\nu_{\perp}=0.57(1)$ [15,16].

For the experiment reported here, we improved the temperature control and limited the x-ray exposure at individual temperatures in order to increase the reduced temperature range accessed during the experiment. We also use a somewhat different analysis method than previously. From these experiments and analyses we conclude that our understanding of the liquid crystal aerosil system needs to be modified; specifically the transition in these model systems is similar to a transition in a system with finite extent. The disorder effect is principally observable in the reduction of the extent of the ordered regions, and in the momentum dependence of the scattering function.

In order to prepare the aerosil–liquid-crystal mixtures, we mixed stoichiometric amounts of hydrophilic aerosil particles (70 Å diameter, purchased from Degussa Corp.) and 4O.8 liquid crystal molecules (purchased from Friton laboratories) with anhydrous ethanol and sonicated the solution for about 60 min. The ethanol was then evaporated slowly. Once dried, a small amount of the mixture was put in an x-ray transparent cell and kept at about 355 K for at least 6 h. This last step ensured that the aerosil–liquid-crystal mixture reached equilibrium at a temperature in the liquid crystal isotropic phase before the start of the x-ray measurements.

X-ray scattering data were collected on the bend magnet beamlines X20A and X22A of the National Synchrotron Light Source of the Brookhaven National Laboratory. The beamlines were set up with Si(111) monochromators and Ge(111) (X20A) or Si(111) (X22A) analyzer crystals. The energy of the incoming x-ray beam was 10.0 keV (X20A) and 10.7 keV (X22A). For the measurements, the sample

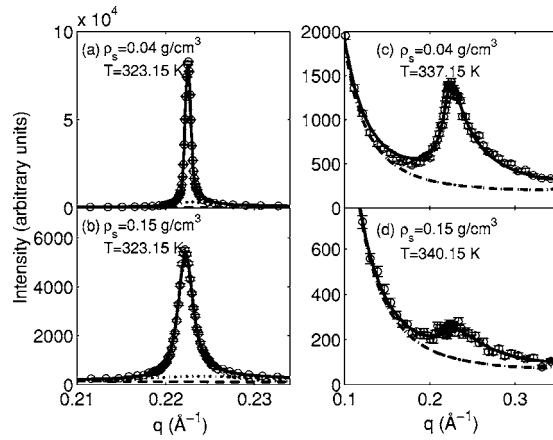


FIG. 1. Scattering intensity for 4O.8-confined aerosil gels. The full curves show the best fit to the model function, the dotted curves show the two individual components of Eq. (1) (in each panel, one of the two components nearly completely overlaps with the full curve), and the dashed curves show the background scattering. (a) and (b) show data taken below the transition temperature T_* while (c) and (d) show data taken above T_* .

cell was placed in an oven at 353 K. Data were collected from this temperature down to 323 K. At each temperature, we collected two scans: a scan of the smectic peak and a scan of the direct beam profile. This latter scan was used to define the resolution function of the spectrometer. We collected between 30 and 40 scans on each sample, limiting the total x-ray exposure to less than two hours. No significant damage to the liquid crystal was observed at that exposure level.

Examples of representative scans of the smectic order peak are shown in Fig. 1. The data analysis of these scans proceeds through nonlinear least squares fits of the data to a model function. All the data collected on a single sample are analyzed simultaneously, allowing for the determination of global parameters common to all scans in addition to parameters specific to a single scan.

The scattering cross section from the liquid crystals contains two terms which describe the thermal (σ_1 term) and random-field (a_2 term) fluctuations of the smectic order.

$$S(\mathbf{q}, T) = \sigma_1(T) L(\mathbf{q}, q_0(T), \xi_{\parallel}(T), \xi_{\perp}(T), \xi_s(T)) + a_2(T) \tilde{\xi}_{\perp}^2 \tilde{\xi}_{\parallel} (L(\mathbf{q}, q_0(T), \tilde{\xi}_{\parallel}, \tilde{\xi}_{\perp}, \tilde{\xi}_s))^2, \quad (1)$$

$$L(\mathbf{q}) = \frac{1}{1 + (q_{\parallel} - q_0)^2 \xi_{\parallel}^2 + q_{\perp}^2 \xi_{\perp}^2 + q_{\perp}^4 \xi_s^4}, \quad (2)$$

where q_{\parallel} and q_{\perp} are the components of the momentum parallel and perpendicular to the smectic wave vector \mathbf{q}_0 . ξ_{\parallel} and ξ_{\perp} are the parallel and perpendicular correlation lengths, and $\xi_s = c^{1/4} \xi_{\perp}$ is the splay correlation length [17]. In Eq. (1), σ_1 , a_2 , q_0 , ξ_{\parallel} , ξ_{\perp} , and ξ_s are temperature-dependent parameters and $\tilde{\xi}_{\parallel}$, $\tilde{\xi}_{\perp}$, and $\tilde{\xi}_s$ are temperature independent. The temperature independence of the random-field term correlation lengths is established empirically. Because the peak profile is rather insensitive to ξ_{\perp} and ξ_s , these two parameters are considered functions of ξ_{\parallel} . Since all three quantities have power-

law dependence relative to the reduced temperature, ξ_s and ξ_{\perp} can also be expressed as power-law functions of ξ_{\parallel} . In this analysis, the power-law parameters for ξ_{\perp} and ξ_s were assumed to be equal to the pure liquid crystal values. In the absence of disorder, the second term would be replaced by a power-law singularity in the smectic-A phase.

In one respect, Eq. (1) differs significantly from the function used previously [9,10,12,13]. The length scales of the two terms are independent of each other while they were assumed previously to be identical. It is not possible to determine which of the two cross section forms better describes the data based on the fit quality. However, the function defined in this Rapid Communication seems to provide a more coherent image of the ordering considering both the heat capacity and the x-ray scattering measurements. Measurements of the heat capacity of these gels [6,18] show that critical-like behaviors of this quantity are observed over a wide reduced temperature range both above and below the transition temperature. It can thus be expected that the correlation length of the thermal fluctuations will similarly show power-law behaviors both above and below the critical temperature. This behavior is impossible if the thermal and random-field correlation lengths are linked together since the correlation length of the random-field term clearly saturates to a large value at low temperature. It should be noted that, except in the immediate vicinity of the transition, the intensity and correlation lengths of the random-field term do not strongly depend on the assumption for the thermal term since below the transition temperature, the thermal term contribution to the total scattering intensity is small. A reanalysis of the 8CB and 8OCB data using the present cross section function would only minimally change the shape of the respective a_2 curves.

In order to calculate the experimental peak profile, an angular average of the cross section is calculated (“powder averaging”) and the resulting function is convoluted with the instrumental resolution function before adding the background contribution. The background function is assumed to be temperature independent as the background scattering mostly originates from the silica aerosil particles, the kapton windows of the cell, and the air. The contribution from the liquid crystal molecules (for example from the isotropic phase) is assumed negligible. This follows the conclusions of Ref. [13] in the study of liquid crystals in anisotropic gels. In the present case, because of the extent of the tails of the peak profile, it is very difficult to determine whether the background scattering is really temperature independent, but satisfactory fits are obtained based on this assumption.

In Fig. 1, panels (a) and (b) show scans taken below the nematic–smectic-A transition temperature. In this regime, the scattering signal is dominated by the Lorentzian square term of the cross section, with the Lorentzian term only providing a marginal contribution. Considering the uncertainty in the determination of the background and the exact peak shape, it is difficult to determine the amplitude and correlation length of the Lorentzian term below the transition, but the data allow for a power-law decrease of the thermal fluctuations in that temperature range, as is the case in a phase transition to long-range order. Above the transition temperature, as Fig. 1(c) and 1(d) show, only a Lorentzian contribution can be

TABLE I. Low-temperature parallel correlation length, low-temperature scattering intensity, transition temperature T_* , and effective exponent β for eight samples of 4O.8 confined to aerosil gels of different densities. For each of the two lowest-density gels, two samples were studied. The gel densities are given as $\rho_s = M_{\text{SiO}_2}/V_{LC}$. The low-temperature scattering intensity (a_2 at 323.15 K) is normalized by the scattering signal of the aerosil particles, b_{SiO_2} .

ρ_s (g/cm ³)	$\tilde{\xi}_{ }$ (Å)	a_{2LT}/b_{SiO_2}	T_* (K)	β
0.025 A	16000(800)	2.80(12)	334.28(3)	0.245(15)
0.025 B	16500(900)	2.29(6)	334.28(3)	0.25(2)
0.040 A	8350(450)	1.71(8)	334.04(2)	0.22(1)
0.040 B	9900(500)	1.77(6)	334.06(2)	0.25(3)
0.062	4100(300)	1.14(2)	333.63(3)	0.23(3)
0.096	3100(300)	0.79(2)	333.37(4)	0.29(4)
0.15	1180(60)	0.423(12)	333.10(10)	0.33(3)
0.30	580(50)	0.247(12)	332.90(30)	0.36(4)

observed. This is similar to what is observed in a phase transition to long range order.

Table I lists the parameters related to the Lorentzian square term of the cross section. The intensity of this second term, a_2 , depends only weakly on the assumptions for the background form, the values of ξ_{\perp} and ξ_s , and the exact shape of the resolution function. The remainder of this Rapid Communication concentrates on this quantity.

a_2 can be considered as the square of the order parameter of the phase transition. a_2 is thus expected to follow a critical-like behavior near the transition temperature. This behavior should be limited to temperatures for which the length scale of the thermal fluctuations is significantly shorter than the low-temperature correlation length. Figures 2 and 3 show a_2 on linear and logarithmic scales for three different aerosil gel densities. In these samples, a power-law behavior is measured down to a reduced temperature t of

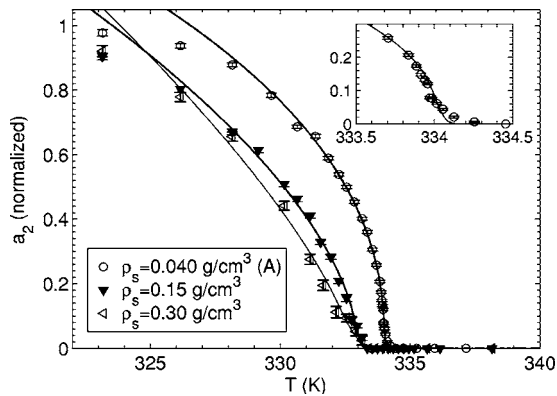


FIG. 2. Plot of the intensity of the scattering signal a_2 as function of the temperature. a_2 is proportional to the square of the order parameter. The full curves are fits to a power law of the form $t^{2\beta}$ with $t = 1 - T/T_*$, and T_* , the transition temperature, is described by a Gaussian distribution to account for the rounding. The inset shows the data near the transition temperature of the $\rho_s = 0.040$ g/cm³ sample.

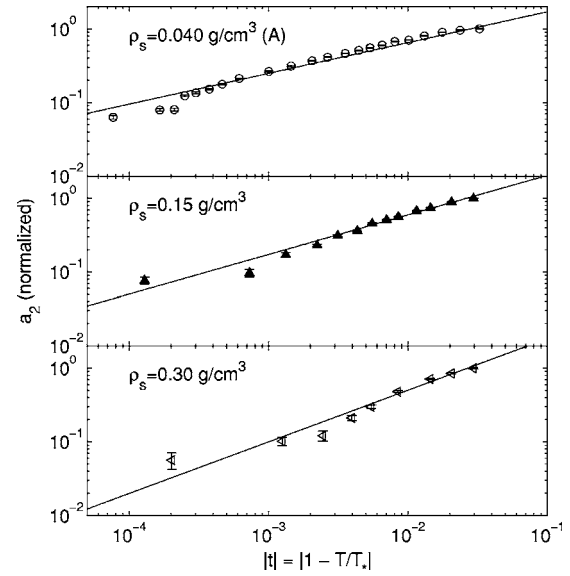


FIG. 3. Plot on a logarithmic scale of the scattering signal a_2 as function of the reduced temperature $t = 1 - T/T_*$. T_* is determined by the best fit of a_2 to the expression $a_0 t^{2\beta}$.

2×10^{-4} ($\rho_s = 0.040$ g/cm³), 1×10^{-3} ($\rho_s = 0.15$ g/cm³), and 5×10^{-3} ($\rho_s = 0.30$ g/cm³). These reduced temperatures can be compared to the lower-bound value imposed by the finite-size domains. Assuming that the correlation lengths in the gels can be estimated with the same power-law equation as in the pure liquid crystal material and that the thermal correlations are identical above and below the transition, the thermal fluctuations would reach the low-temperature correlation lengths measured in these gels at $t = 2.3 \times 10^{-5}$, 3.7×10^{-4} , and 1.0×10^{-3} , respectively. These values are three to eight times smaller than the values measured experimentally. A similar conclusion on the magnitude of the temperature rounding has been reached from the heat capacity data on octylcyanobiphenyl-aerosil samples [18,19]. The temperature range in which we observe power-law behaviors satisfies the range expected for a transition in a finite-size system (note that some of the rounding could be due to inhomogeneities or to the disconnected susceptibility).

Fits of the a_2 curves to power-law forms can be used to determine the effective order parameter critical exponent β ($a_2 \sim t^{2\beta}$). As shown in the top panel of Fig. 4, β increases with increasing disorder toward the value calculated for the 3D XY model. This behavior is similar to the evolution of the critical exponents with the McMillan ratio ($R_M = T_{NA}/T_{IN}$) in pure liquid crystals [20]. In samples with aerosil dispersion, an effective McMillan ratio R_M^* can be calculated: $R_M^*(4O.8, \rho_s) = R_M(4O.8) - m_\rho \rho_s$, where $R_M(4O.8) = 0.958$ and $m_\rho = 0.45 \pm 0.10$. The linear relationship between the effective McMillan ratio and the aerosil density was previously observed with the heat capacity exponent α for 4O.8 and 8CB liquid crystals [6,18], and with the order parameter exponent β for 8CB liquid crystals [10]. The same value of m_ρ (0.45 ± 0.10) is found in all cases. As the McMillan ratio characterizes the strength of the coupling between the nematic and smectic order parameters, increasing disorder seems to effectively decrease the nematic susceptibility.

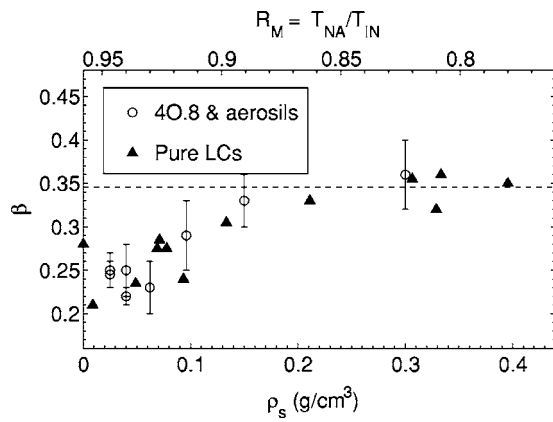


FIG. 4. Value of the effective power-law exponent β as function of the aerosil gel density. Also shown are the values of β calculated from the Rushbrooke relation ($2\beta = 2 - \alpha - \gamma$) for pure liquid crystal transitions as a function of the McMillan ratio ($R_M = T_{NA}/T_{IN}$, where T_{NA} and T_{IN} are the N -SmA and I -N transition temperatures). These values are tabulated in Ref. [20]. The dashed line shows the value of β calculated for the 3D XY model.

Finally, the low-temperature values of a_2 normalized by the scattering intensity of the aerosil network b_{SiO_2} are listed in Table I (the silica particle scattering is determined from the background with a term of the form $1/q^{3.8}$ [7]).

a_2/b_{SiO_2} is proportional to $1/\rho_s$. The scattering strength is thus simply proportional to the liquid crystal mass in the x-ray beam path.

In conclusion, the study of the liquid crystal 4O.8 confined in aerosil gels shows that, at weak disorder, liquid crystals order in a short-range smectic state in a way similar to that of a finite-size system. The data are qualitatively similar to the results obtained on 8CB-aerosil mixtures. Thus, the strength of the disorder created by the aerosil network does not seem to depend strongly on the monomeric or bilayer nature of the smectic phase. The absence of long-range order is consistent with ideas based on the random field 3D XY model but the explicit observed nature of the fluctuations requires further development of the theory. Additional experiments on other liquid crystals to determine the universality of the behavior we observe here would also be invaluable.

We would like to thank K. J. Thomas and J. L. Jordan-Sweet for their assistance, and C. W. Garland and G. S. Iannacchione for helpful discussions. This work was supported by the Natural Science and Engineering Research Council of Canada. Use of the National Synchrotron Light Source, Brookhaven National Laboratory, was supported by the U.S. Department of Energy, Office of Science, Office of Basic Energy Sciences, under Contract No. DE-AC02-98CH10886.

- [1] J. D. Reppy, *J. Low Temp. Phys.* **87**, 205 (1992).
- [2] D. T. Sprague, T. M. Haard, J. B. Kycia, M. R. Rand, Y. Lee, P. J. Hamot, and W. P. Halperin, *Phys. Rev. Lett.* **75**, 661 (1995).
- [3] B. J. Frisken and D. S. Cannell, *Phys. Rev. Lett.* **69**, 632 (1992).
- [4] L. Wu, B. Zhou, C. W. Garland, T. Bellini, and D. W. Schaefer, *Phys. Rev. E* **51**, 2157 (1995).
- [5] T. Bellini, L. Radzihovsky, J. Toner, and N. A. Clark, *Science* **294**, 1074 (2001).
- [6] H. Haga and C. W. Garland, *Phys. Rev. E* **56**, 3044 (1997).
- [7] G. S. Iannacchione, C. W. Garland, J. T. Mang, and T. P. Rieker, *Phys. Rev. E* **58**, 5966 (1998).
- [8] T. Jin and D. Finotello, *Phys. Rev. Lett.* **86**, 818 (2001).
- [9] S. Park, R. L. Leheny, R. J. Birgeneau, J.-L. Gallani, C. W. Garland, and G. S. Iannacchione, *Phys. Rev. E* **65**, 050703(R) (2002).
- [10] R. L. Leheny, S. Park, R. J. Birgeneau, J.-L. Gallani, C. W. Garland, and G. S. Iannacchione, *Phys. Rev. E* **67**, 011708 (2003).
- [11] Z. Kutnjak, S. Kralj, G. Lahajnar, and S. Žumer, *Phys. Rev. E* **70**, 051703 (2004).
- [12] P. S. Clegg, C. Stock, R. J. Birgeneau, C. W. Garland, A. Roshi, and G. S. Iannacchione, *Phys. Rev. E* **67**, 021703 (2003).
- [13] D. Liang, M. A. Borthwick, and R. L. Leheny, *J. Phys.: Condens. Matter* **16**, S1989 (2004).
- [14] L. Radzihovsky and J. Toner, *Phys. Rev. B* **60**, 206 (1999).
- [15] R. J. Birgeneau, C. W. Garland, G. B. Kasting, and B. M. Ocko, *Phys. Rev. A* **24**, 2624 (1981).
- [16] K. J. Stine and C. W. Garland, *Phys. Rev. A* **39**, 3148 (1989).
- [17] W. G. Bouwman and W. H. de Jeu, *Phys. Rev. Lett.* **68**, 800 (1992).
- [18] G. S. Iannacchione, S. Park, C. W. Garland, R. J. Birgeneau, and R. L. Leheny, *Phys. Rev. E* **67**, 011709 (2003).
- [19] In Ref. [7], two different length scales are considered for the finite-size analysis: the average void length of the gel (FSS: finite-size scaling) and the low-temperature correlation lengths of the smectic order as measured by x-ray scattering (RFS: random-field scaling). Only the second of these length scales is considered here.
- [20] C. W. Garland and G. Nounesis, *Phys. Rev. E* **49**, 2964 (1994).